Physica A 167 (1990) 361–383
North-Holland

COMPUTER SIMULATIONS OF NEAREST-NEIGHBOR DISTRIBUTION FUNCTIONS AND RELATED QUANTITIES FOR HARD-SPHERE SYSTEMS

S. TORQUATO

Department of Mechanical and Aerospace Engineering, and Department of Chemical Engineering, North Carolina State University, Raleigh, NC 27695-7910, USA

Sang Bub LEE[1]

Department of Mechanical and Aerospace Engineering, North Carolina State University, Raleigh, NC 27695-7910, USA

Received 4 January 1990
Revised manuscript received 13 March 1990

One of the fundamental quantities which statistically characterizes a random system of interacting particles is the nearest-neighbor distribution function. We present computer-simulation results for *two different* types of nearest-neighbor distribution functions for random distributions of identical impenetrable (hard) spheres. We also report, for such systems, computer-simulation data for closely related quantities such as the associated cumulative distributions. From this information, we calculate the "mean nearest-neighbor distance" between particles. Our computer-simulation results are compared to the various sets of theoretical expressions derived recently by Torquato, Lu and Rubinstein. One of these sets of expressions is shown to be in excellent agreement with the simulation data.

1. Introduction

One of the basic statistical quantities characterizing a random system of interacting particles is the nearest-neighbor distribution function H_P, i.e., the probability density function associated with finding a *nearest neighbor* at some given distance from a reference particle. Knowledge of H_P is of importance in a host of problems, including the structure and properties of liquids and amorphous solids [1–4], flow of suspensions [5], flow in porous media [6, 7], diffusion-controlled reactions in heterogeneous media [8, 9], and stellar dynamics [10], to mention but a few examples. It was Hertz [11] who apparently was the first to consider its evaluation for "point" particles. It is only recently [12] that a

[1] Present and permanent address: Department of Physics Education, Kyungpook National University, Daegu 701-702, Korea.

theory has been developed to represent and compute H_P for systems of interacting, finite-sized particles. It should be emphasized that H_P is *different* from the well known radial distribution function, the latter being proportional to the probability of finding any particle (not necessarily the nearest one) at a distance r away from the central particle.

A different nearest-neighbor distribution function, H_V, arises in the scaled-particle theory of liquids [13]. This function (defined more precisely in the subsequent section) essentially characterizes the probability of finding a nearest-neighbor particle at a given distance from a point in the void region, i.e., the region exterior to the particles. The quantities H_P and H_V are referred to as "particle" and "void" nearest-neighbor distribution functions, respectively. In addition to the nearest-neighbor distribution functions there are the closely related exclusion probability functions, E_P and E_V, and conditional pair distribution functions, G_P and G_V, which are equally important statistical descriptors of the microstructure.

This paper has a twofold purpose: 1) to develop an algorithm to compute the aforementioned nearest-neighbor and related functions for random distributions of impenetrable (hard) spheres from computer simulations; and 2) compare the resulting data with the recent corresponding theoretical expressions derived by Torquato, Lu and Rubinstein [12] for such models.

In section 2, we define the basic quantities and key theoretical results of Torquato et al. In section 3, we describe our simulation procedure. In section 4, we present computer-simulation results for point particles and thus demonstrate the accuracy of the simulation technique. In section 5, we present computer-simulation results for the *void* nearest-neighbor distribution and related functions for impenetrable-sphere systems and compare the results to theory. In section 6, we report corresponding computer-simulation results for the *particle* quantities and the mean nearest-neighbor distance between particles, and again compare them to theory. In section 7. we make concluding remarks.

2. Summary of theory

Here we shall summarize only some of the basic theoretical relations for the nearest-neighbor distribution functions and related quantities for random distributions of identical D-dimensional spheres obtained by Torquato, Lu and Rubinstein [12]. Although many of their results apply to inhomogeneous systems, we shall restrict the following discussion to statistically isotropic systems of spheres (with $D = 3$) since our simulations are carried out for isotropic hard-sphere and penetrable-sphere systems.

2.1. Definitions and basic relations

Consider a random distribution of identical spheres of diameter σ at number density ρ. We want to study two different types of nearest-neighbor distribution functions, $H_V(r)$ and $H_P(r)$, defined as follows:

$H_V(r)\,dr$ = Probability that at an arbitrary point in the system the center of the nearest particle lies at a distance between r and $r + dr$, (1)

$H_P(r)\,dr$ = Given any D-dimensional sphere of diameter σ at some arbitrary position in the system, the probability of finding the center of the nearest particle at a distance between r and $r + dr$. (2)

H_V and H_P are referred to as "void" and "particle" nearest-neighbor distribution functions, respectively. We refer to $H_V(r)$ as *void* nearest-neighbor distribution function since it provides a measure of the probability associated with finding the nearest particle at a distance r from a spherical *cavity* centered in the void region (when $r \geq \sigma/2$), i.e., the region exterior to the spheres. $H_P(r)$ is termed a *particle* nearest-neighbor distribution function since it is the probability density associated with finding the nearest particle at a distance r from an actual particle at the origin. The void nearest-neighbor distribution function defined here is identical to the one defined in the scaled-particle theory of Reiss et al. [13]. The distinction between H_V and H_P, however, has heretofore not been made. Indeed, in the past, these functions have been incorrectly thought to be identical to one another. Note that since both of these functions are probability density functions, they have dimensions of inverse length.

It is useful to introduce "exclusion" probabilities $E_V(r)$ and $E_P(r)$ defined as follows:

$E_V(r)$ = Probability of finding a region Ω_V, which is a D-dimensional spherical cavity of radius r (centered at some arbitrary point) empty of particle centers

= Probability of inserting a "test" particle of radius $r - \sigma/2$ (at some arbitrary position) in the system of spheres, (3)

$E_P(r)$ = Given any D-dimensional sphere at some arbitrary position, the probability of finding a region Ω_P, which is a sphere of radius r encompassing this central particle, empty of particle centers. (4)

Observe that the first and second lines of (3) are equivalent since the region excluded to a particle center of radius $\sigma/2$ by a "test" particle of radius $r-\sigma/2$ is a sphere of radius r. The *test* particle serves to probe the void region. It follows that the exclusion probabilities are related to the nearest-neighbor distribution by the expressions

$$E_V(r) = 1 - \int_0^r H_V(x)\,dx \tag{5}$$

and

$$E_P(r) = 1 - \int_0^r H_P(x)\,dx\,. \tag{6}$$

The integrals of (5) and (6) respectively represent the probabilities of finding at least one particle center in regions Ω_V and Ω_P. Differentiating the exclusion-probability relations with respect to r gives

$$H_V(r) = \frac{-\partial E_V(r)}{\partial r} \tag{7}$$

and

$$H_P(r) = \frac{-\partial E_P(r)}{\partial r}\,. \tag{8}$$

It is useful to write the nearest-neighbor distribution functions as a product of two different correlation functions:

$$H_V(r) = \rho 4\pi r^2 G_V(r)\, E_V(r) \tag{9}$$

and

$$H_P(r) = \rho 4\pi r^2 G_P(r)\, E_P(r)\,. \tag{10}$$

Given definitions (1)–(4), the *conditional* "pair" distribution functions, G_V and G_P, must have the following interpretations:

$$\rho 4\pi r^2 G_V(r)\,dr = \text{Given that region } \Omega_V \text{ (spherical cavity of radius } r\text{) is empty of particle centers, the probability of finding particle centers in the spherical shell of volume } 4\pi r^2\,dr \text{ encompassing the cavity,} \tag{11}$$

$\rho 4\pi r^2 G_P(r)\,dr$ = Given that region Ω_P (sphere of radius r encompassing any particle centered at some arbitrary position) is empty of particle centers, the probability of finding particle centers in the spherical shell of volume $4\pi r^2\,dr$ surrounding the central particle. (12)

Note that $G_V(r)$ is simply the "radial" distribution function for the "test" particle (of radius $r - \sigma/2$) and a particle (of radius $\sigma/2$) at contact, i.e., when this pair of particles is separated by the distance r (cf. eq. (3)). Equations (9) and (10) may be regarded as definitions of G_V and G_P, respectively. When $r = \sigma$, then $G_V(\sigma) = G_P(\sigma)$ is just the standard radial distribution function $g_2(\sigma)$ for identical spheres at contact, i.e., at an interparticle separation of σ. Also as $r \to \infty$, the sphere of radius r (in either the *void* or *particle* problems) may be regarded as a plane rigid wall relative to the particles and, in particular, to the particles in contact with wall, hence $G_V(\infty) = G_P(\infty)$. To summarize, G_V and G_P are identical when $r = \sigma$ and $r = \infty$. We know generally they are not the same for $r \leqslant \sigma$ (cf. (20) and (25)); but are they identical for $r \geqslant \sigma$? This interesting question will be answered shortly.

The exclusion probabilities are related to the pair distribution functions via the expressions

$$E_V(r) = \exp\left(-\int_0^r \rho 4\pi y^2 G_V(y)\,dy\right), \tag{13}$$

$$E_P(r) = \exp\left(-\int_0^r \rho 4\pi y^2 G_P(y)\,dy\right), \tag{14}$$

which are obtained by use of (7)–(10). Combination of (7), (8), (13), and (14) yields

$$H_V(r) = \rho 4\pi r^2 G_P(r) \exp\left(-\int_0^r \rho 4\pi y^2 G_V(y)\,dy\right) \tag{15}$$

and

$$H_P(r) = \rho 4\pi r^2 G_P(r) \exp\left(-\int_0^r \rho 4\pi y^2 G_P(y)\,dy\right). \tag{16}$$

Thus, one can calculate the nearest-neighbor distribution functions given either the exclusion probability functions (cf. (7) and (8)) or the pair distribution functions (cf. (15) and (16)).

From $H_P(r)$ one can obtain other quantities of fundamental interests such as the "mean nearest-neighbor distance" l between particles and the random-close packing density. The former is defined as

$$l = \int_0^\infty r H_P(r)\, dr . \tag{17}$$

An operational definition for the random close-packing density then follows: the density at which $l \to \sigma$.

Calculations of the nearest-neighbor distribution functions and the auxiliary quantities, the exclusion probabilities and conditional pair distribution functions, are generally nontrivial for mutually impenetrable particles of diameter σ. However, for such a model, one can state exact relations for certain small ranges of r. For instance it is clear from the definitions (2) and (6) that

$$E_P(r) = 1 \qquad \text{for } 0 \leq r \leq \sigma , \tag{18}$$

$$H_P(r) = 0 \qquad \text{for } 0 \leq r \leq \sigma , \tag{19}$$

$$G_P(r) = 0 \qquad \text{for } 0 \leq r \leq \sigma , \tag{20}$$

because one particle excludes another from occupying the same space.

Futhermore, in the case of the *void* problem, a spherical cavity of radius r and volume $4\pi r^3/3$ can contain at most one particle center if $r \leq \sigma/2$. Thus, for statistically homogeneous media, the exclusion probability is then given by

$$E_V(r) = 1 - \rho \frac{4\pi r^3}{3} \qquad \text{for } 0 \leq r \leq \sigma/2 , \tag{21}$$

and hence by (7) we also have

$$H_V(r) = \rho 4\pi r^2 \qquad \text{for } 0 \leq r \leq \sigma/2 . \tag{22}$$

For $r \leq \sigma/2$, $\rho 4\pi r^3/3$ is just the probability that the cavity of radius r is occupied and hence $E_V(r)$ is just one minus this latter quantity. Note that for $r < \sigma/2$, the test particle may be regarded as a "point" particle that is capable of penetrating the mutually impenetrable particles. Hence, for $r < \sigma/2$, decreasing r then increases E_V, according to eq. (21), until E_V reaches its maximum value of unity at $r = 0$. Note that for $r = \sigma/2$,

$$E_V(\sigma/2) = 1 - \eta = 1 - \phi_2 = \phi_1 , \tag{23}$$

where

$$\eta = \rho\pi\sigma^3/6 \tag{24}$$

is a reduced density which, in the case of hard spheres only, is equal to the particle volume fraction ϕ_2. Therefore, $\phi_1 = 1 - \phi_2$ is just the *void* volume fraction. From eqs. (9), (21) and (22), one also has

$$G_V(r) = \frac{1}{1 - \rho 4\pi r^3/3} \qquad \text{for } 0 \leqslant r \leqslant \sigma/2 . \tag{25}$$

For particles which can overlap one another, relations (18)–(22) and (25) will not hold. Moreover, for overlapping particles, $\eta \neq \phi_2$, i.e., the reduced density η is *not equal* to the sphere volume fraction ϕ_2. These points shall be elaborated upon shortly.

2.2. Relationship between void and particle quantities

Although the void and particle quantities are not the same for $r < \sigma$, they are in fact related to one another for $r \geqslant \sigma$ in the case of a *statistically homogeneous* medium of hard spheres. Torquato et al. [12] found that for such hard-sphere systems

$$E_P(r) = \frac{E_V(r)}{E_V(\sigma)} , \qquad r \geqslant \sigma . \tag{26}$$

Combination of (26) with (7) and (8) gives the following expressions relating the different nearest-neighbor distribution functions:

$$H_P(r) = \frac{H_V(r)}{E_V(\sigma)} , \qquad r \geqslant \sigma . \tag{27}$$

From (9) and (10) one exactly has

$$\frac{G_P(r)}{G_V(r)} = \frac{H_P(r)}{H_V(r)} \frac{E_V(r)}{E_V(r)} , \qquad r \geqslant \sigma . \tag{28}$$

Combination of (26), (27) and (28) then yields

$$G_P(r) = G_V(r) , \qquad r \geqslant \sigma . \tag{29}$$

For isotropic, equilibrium distributions of hard spheres, Reiss et al. [13] related the *void* pair distribution function at $r = \sigma$ to this function at $r = \infty$. This relation combined with eq. (29) then yields

$$G_V(\infty) = G_P(\infty) , \tag{30}$$

where

$$G_V(\infty) = 1 + 4\eta G_V(\sigma)\,, \tag{31}$$

$$G_P(\infty) = 1 + 4\eta G_P(\sigma)\,, \tag{32}$$

for such hard-sphere systems. Note that (31) and (32) are the dimensionless equations of state [14] for hard spheres, i.e.,

$$G_V(\infty) = G_P(\infty) = \frac{p}{\rho kT}\,, \tag{33}$$

where p is the pressure, T is temperature, and k is Boltzmann's constant.

2.3. *Relations for arbitrary density*

Torquato et al. [12] have derived exact integral representations of all of the aforementioned functions for homogeneous distributions of identical D-dimensional spheres of diameter σ which interact with an *arbitrary potential* in terms of the n-particle probability density functions $\rho_1, \ldots, \rho_n$. The quantity $\rho_n(\boldsymbol{r}_1, \ldots, \boldsymbol{r}_n)$ characterizes the probability of finding a configuration of n spheres with positions $\boldsymbol{r}_1, \ldots, \boldsymbol{r}_n$, respectively.

2.3.1. *Fully penetrable spheres*

For spatially uncorrelated spheres (Poisson distributed centers) or *fully penetrable spheres*, $\rho_n = \rho^n$ and the aforementioned expressions lead to the results first obtained by Hertz [11]:

$$H_V(r) = H_P(r) = \rho 4\pi r^2 \exp\left(\frac{-\rho 4\pi r^3}{3}\right), \tag{34}$$

$$E_V(r) = E_P(r) = \exp\left(\frac{-\rho 4\pi r^3}{3}\right), \tag{35}$$

$$G_V(r) = G_P(r) = 1\,. \tag{36}$$

Note that the *void* and *particle* quantities become identical for fully penetrable spheres, as expected.

2.3.2. *Impenetrable spheres*

For three-dimensional impenetrable spheres (as well as two-dimensional), the two-particle probability density ρ_2 is only known approximately for arbitrary density, albeit accurately [14]; the higher-order ρ_n ($n \geq 3$) are generally

never known. This implies that the integral series representations of the void and particle quantities derived by Torquato et al. [12] cannot be evaluated exactly for such models. Torquato et al. thus developed approximate relations for these functions which amount to approximately summing the aforementioned series representations. They derived *three different sets* of approximate relations for the void quantities and then obtained corresponding relations for the particle quantities via the "connection" equations (26), (27) and (29).

Scaled-particle approximations of the *void* quantities were obtained by Reiss et al. [13]:

$$\sigma H_V(x) = 24\eta(1-\eta)(ax^2 + bx + c)\exp[-\eta(8ax^3 + 12bx^2 + 24cx + d)], \quad x > \tfrac{1}{2}, \tag{37}$$

$$E_V(x) = (1-\eta)\exp[-\eta(8ax^3 + 12bx^2 + 24cx + d)], \quad x > \tfrac{1}{2}, \tag{38}$$

$$G_V(x) = a + \frac{b}{x} + \frac{c}{x^2}, \quad x > \tfrac{1}{2}. \tag{39}$$

Here $x = r/\sigma$ and a, b, and c are the density-dependent coefficients given by

$$a(\eta) = \frac{1 + \eta + \eta^2}{(1-\eta)^3}, \tag{40}$$

$$b(\eta) = \frac{-3\eta(1+\eta)}{2(1-\eta)^3}, \tag{41}$$

$$c(\eta) = \frac{3\eta^2}{4(1-\eta)^3}. \tag{42}$$

Torquato et al. [12] then used these relations in conjunction with eqs. (26), (27) and (29) to obtain, for the first time, the *particle* quantities in the scaled-particle approximation:

$$\sigma H_P(x) = 24\eta(ax^2 + bx + c) \times \exp\{-\eta[8a(x^3 - 1) + 12b(x^2 - 1) + 24c(x-1)]\}, \quad x > 1, \tag{43}$$

$$E_P(x) = \exp\{-\eta[8a(x^3 - 1) + 12b(x^2 - 1) + 24c(x-1)]\}, \quad x > 1, \tag{44}$$

$$G_P(x) = a + \frac{b}{x} + \frac{c}{x^2}, \quad x > 1. \tag{45}$$

Two additional sets of approximations for the *void* were found by Torquato et al. by exploiting the observation made earlier, namely that $G_V(r)$ is just the contact radial distribution function for a test particle of radius $r - \sigma/2$ (at infinite dilution) and an actual particle of diameter σ. This was done [12] by employing the relation for the contact radial distribution function for general *binary* mixtures of hard spheres in the aforementioned limit in both the Percus–Yevick and Carnahan–Starling approximations. In the Percus–Yevick approximation, Torquato et al. found that the *void* and *particle* quantities are given by

$$\sigma H_V(x) = \frac{24\eta}{(1-\eta)}\left[(1+2\eta)x^2 - \tfrac{3}{2}\eta x\right] \times \exp\left(\frac{\eta}{(1-\eta)^2}\left[8(1+2\eta)x^3 - 18\eta x^2 + \tfrac{5}{2}\eta - 1\right]\right), \quad x > \tfrac{1}{2}, \tag{46}$$

$$E_V(x) = (1-\eta)\exp\left(-\frac{\eta}{(1-\eta)^2}\left[8(1+2\eta)x^3 - 18\eta x^2 + \tfrac{5}{2}\eta - 1\right]\right), \quad x > \tfrac{1}{2}, \tag{47}$$

$$G_V(x) = \frac{(1+2\eta-3\eta/2x)}{(1-\eta)^2}, \qquad x > \tfrac{1}{2}, \tag{48}$$

$$\sigma H_P(x) = \frac{24\eta}{(1-\eta)^2}\left[(1+2\eta)x^2 - \tfrac{3}{2}\eta x\right] \times \exp\left(\frac{-\eta}{(1-\eta)^2}\left[8(1+2\eta)(x^3-1) - 18\eta(x-1)\right]\right), \quad x > 1, \tag{49}$$

$$E_P(x) = \exp\left(\frac{-\eta}{(1-\eta)^2}\left[8(1+2\eta)(x^3-1) - 18\eta(x-1)\right]\right), \qquad x > 1, \tag{50}$$

$$G_P(x) = \frac{(1+2\eta-3\eta/2x)}{(1-\eta)^2}, \qquad x > 1. \tag{51}$$

In the Carnahan–Starling approximation, it was found [12] that the *void* and *particle* quantities are given by

$$H_V(x) = 24\eta(1-\eta)(ex^2 + fx + g)\exp[-\eta(8ex^3 + 12fx^2 + 24gx + h)], \quad x > \tfrac{1}{2}, \tag{52}$$

$$E_V(x) = (1-\eta)\exp[-\eta(8ex^3 + 12fx^2 + 24gx + h)], \qquad x > \tfrac{1}{2}, \tag{53}$$

$$G_V(x) = e + \frac{f}{x} + \frac{g}{x^2}, \qquad x > \tfrac{1}{2}, \tag{54}$$

$$H_P(x) = 24\eta[ex^2 + fx + g] \times \exp\{-\eta[8e(x^3 - 1) + 12f(x^2 - 1) + 24g(x - 1)]\}, \quad x > 1, \tag{55}$$

$$E_P(x) = \exp\{-\eta[8e(x^3 - 1) + 12f(x^2 - 1) + 24g(x - 1)]\}, \quad x > 4, \tag{56}$$

$$G_P(x) = e + \frac{f}{x} + \frac{g}{x^2}, \quad x > 1, \tag{57}$$

where

$$e(\eta) = \frac{1 + \eta}{(1 - \eta)^3}, \tag{58}$$

$$f(\eta) = -\frac{\eta(3 + \eta)}{2(1 - \eta)^3}, \tag{59}$$

$$g(\eta) = \frac{\eta^2}{2(1 - \eta)^3}, \tag{60}$$

$$h(\eta) = \frac{-9\eta^2 + 7\eta - 2}{2(1 - \eta)^3}. \tag{61}$$

3. Simulation procedure

Here we shall describe the simulation procedure we employed to compute the exclusion probabilities, E_V and E_P, and the nearest-neighbor distribution functions, H_V and H_P. We do not directly simulate the conditional pair distribution functions since: (i) simulations of G_V and G_P require substantial computational time to reduce the larger statistical fluctuations which arise; and (ii) they can be obtained from knowledge of the exclusion probabilities and nearest-neighbor distribution functions via eqs. (9) and (10) or through eqs. (13)–(16). The simulation procedure consists of two basic steps: (i) generating equilibrium realizations or configurations of the random medium; and (ii) sampling the desired quantities.

We employed a conventional Metropolis algorithm [14] to generate equilibrium distributions of both fully penetrable and totally impenetrable spheres of diameter σ. Particles were initially placed in a cubical system of volume L^3 on the sites of a body-centered cubic array. The system was surrounded by periodic images of itself, i.e., periodic boundary conditions were employed. For impenetrable-particle systems, the model of prime interest, each particle was moved (by some small distance) to a new position, provided that no

overlap occurred; this process was repeated until equilibrium was achieved. For penetrable-particle systems, each particle was moved without regard to overlap; this process was repeated until the centers were Poisson distributed. Since the exact analytical results (34)–(36) are known for penetrable spheres, this model serves as a useful test case.

In generating hard-sphere configurations, we employed the "cell-list" method [15] to efficiently check for overlap among the particles. Specifically, the system volume was subdivided into cubic cells, each having a side of length slightly smaller than $\sigma/\sqrt{3}$; thus, each cell contained at most one sphere center. Each time a particle was moved to a randomly chosen point, we checked for overlap by first determining the cell in which the new position fell in. If the cell already contained a sphere center, then that current attempt was discarded. If the cell did not contain a sphere center, then the overlap condition was tested between the new position and the particles in the neighboring cell. Since the diameter of each particle is greater than the side of each cell, we only needed to test the overlap condition in the eight nearest-neighbor cells. If the new position is allowed, then the coordinates of the center of the moving particle are updated with those of the new position. This process was repeated for each particle until equilibrium was achieved.

Our simulations were carried out for 500-particle systems for various values of the reduced density $\eta = \rho\pi\sigma^3/6$. This system size was found to be large enough to eliminate finite-size effects. Each of our simulations, depending upon η, consisted of 10 000–60 000 moves per particle, the first 200–400 of which were discarded before sampling for equilibrium statistical measures. Realizations were selected every 10–50 moves per particle, again depending upon the value of η.

Let us now describe the sampling methods for the exclusion probabilities and nearest-neighbor distribution functions.

3.1. *Sampling for E_P and E_V*

The sampling techniques used to measure E_P and E_V are very similar. First consider the determination of E_P. For jth configuration, we surrounded each sphere in the central system with concentric spherical shells of radii

$$r_i = i\,\Delta r\,, \qquad i = 1, 2, 3, \ldots \tag{62}$$

and thickness Δr (where $\Delta r \ll \sigma$). For a particular value of r_i, we then determined the total number of situations $N_0^{(j)}$ in which no sphere centers lie in concentric shells of inner radius σ and outer radius r_i surrounding each sphere. Let $N_t^{(j)}$ denote the total number of shells of radius r_i sampled for the jth

configuration and M denote the total number of configurations. Then, according to (4), the particle exclusion probability is algorithmically equivalent to

$$E_{\mathrm{P}}(r) = \frac{1}{m} \sum_{j=1}^{M} \frac{N_0^{(j)}}{N_{\mathrm{t}}^{(j)}} . \tag{63}$$

The simulation method for the *void* exclusion probability $E_{\mathrm{V}}(r)$ is the same except for the fact that here a randomly chosen point (instead of an actual sphere) lies at the center of the concentric shells.

3.2. Sampling for H_{P} and H_{V}

The sampling methods used to measure H_{P} and H_{V} are related to the ones employed to measure the exclusion probabilities and hence simulation of the former can be done concurrently with the latter. Let us first consider H_{P}. As in the case of obtaining E_{P}, we constructed concentric spherical shells of radii r_i (cf. eq. (62)) and thickness Δr around each sphere in the jth realization. One then determines the total number of nearest-neighbor particles contained in the shells of radius r_i, $N_{\mathrm{n}}^{(j)}$, i.e., one determines which shells of radius r_i are the innermost occupied shells and then counts the total number of particles contained in such shells. Hence, according to (2), we have that

$$H_{\mathrm{P}}(r_i)\,\Delta r = \frac{1}{M} \sum_{j=1}^{M} \frac{N_{\mathrm{n}}^{(j)}}{N_{\mathrm{t}}^{(j)}} . \tag{64}$$

In order for (64) to yield accurate results, Δr must be chosen to be much smaller than σ. For our simulations, we chose $0.00125\sigma \leqslant \Delta r \leqslant 0.0025\sigma$. The cell-list method was also used here to efficiently count the number of nearest-neighbor particles. The simulation technique for the *void* nearest-neighbor distribution function $H_{\mathrm{V}}(r)$ is the same except that here a randomly chosen point lies at the center of the concentric shells.

In the subsequent sections, we shall report our simulation results and compare these data to the aforementioned theoretical expressions in various figures. Since the density of simulation points is quite large, we will only report a subset of those data in order to distinguish the data from the theory. Our hard-sphere data will include cases up to $\eta = \phi_2 = 0.5$. At about this volume fraction, the equilibrium hard-sphere system undergoes a fluid–solid phase transition [14]. Simulations of hard-sphere systems for ϕ_2 between 0.5 and the random-close packing fraction (estimated [2] to range between 0.62–0.66) are quite subtle [3] and shall be examined in a future work.

4. Results for fully penetrable spheres

As indicated earlier, the instance of fully penetrable spheres (randomly centered spheres) provides a useful test case of our simulation technique since for such a system we have the exact results (34)–(36). Specifically, we have determined the exclusion probability function and the nearest-neighbor distribution function for a system of fully penetrable spheres at a reduced number density $\eta = 0.7$. For such distributions, $\eta \neq \phi_2$, unlike the case of impenetrable spheres, but η is related to ϕ_2 through the relation

$$\phi_2 = 1 - \exp(-\eta) . \tag{65}$$

Since there is no distinction between the *void* and *particle* quantities for randomly centered spheres, $E(r)$ shall denote $E_P(r) = E_V(r)$ and $H(r)$ shall denote $H_P(r) = H_V(r)$. In fig. 1, we show our simulation data for the dimensionless nearest-neighbor distribution function $\sigma H(r)$ and the exact result (34). Fig. 2 depicts our simulation results for the exclusion probability $E(r)$ as well as the corresponding exact result (35). From figs. 1 and 2, it is seen that the simulation results for $H(r)$ and $E(r)$ are in excellent agreement with the corresponding exact results.

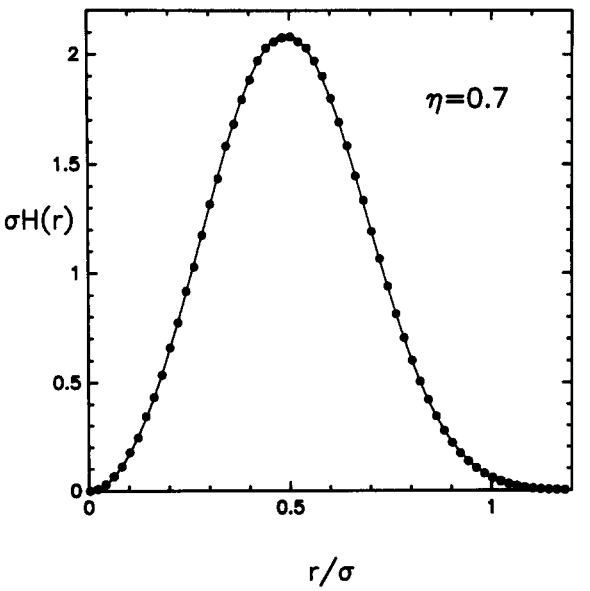

Fig. 1. The dimensionless nearest-neighbor distribution function $\sigma H(r)$ for a distribution of fully penetrable spheres of diameter σ at a reduced density $\eta = 0.7$ ($\phi_2 \simeq 0.5$). Circles are our simulation data and the solid line is obtained from the exact result (34). Here $\eta = \rho\pi\sigma^3/6$, ρ is the number density, and the sphere volume fraction is $\phi_2 = 1 - \exp(-\eta)$.

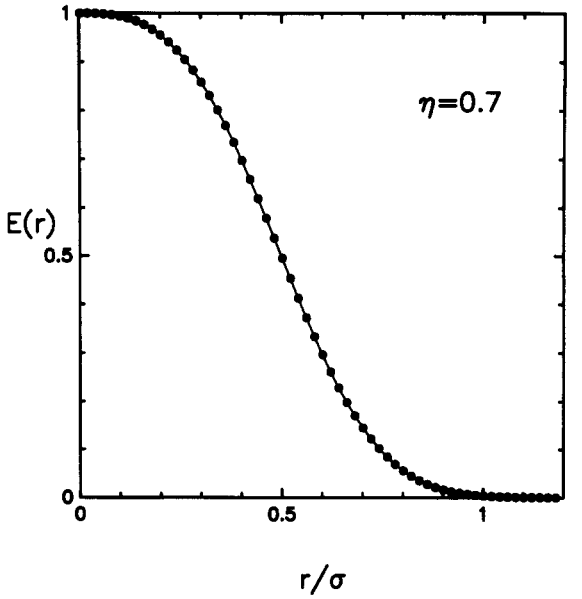

Fig. 2. The exclusion probabilty $E(r)$ for a distribution of fully penetrable spheres of diameter σ at a reduced density $\eta = 0.7$ ($\phi_2 \simeq 0.5$). Circles are our simulation data and the solid line is the exact result (35). Here $\eta = \rho\pi\sigma^3/6$, ρ is the number density, and the sphere volume fraction is $\phi_2 = 1 - \exp(-\eta)$.

5. Results for impenetrable spheres: void quantities

Here we shall report our simulation results for the *void* quantities, H_V and E_V, in the cases of hard spheres. One of our aims will be to ascertain which of the aforementioned three approximations for the void quantities best agrees with the simulation data. We have carried out simulations for $\phi_2 = \eta = 0.1$, 0.2, 0.3, 0.4, and 0.5. For reasons which will soon become apparent, we will only need to explicitly report results for $\phi_2 = 0.2$ and 0.5.

First it is important to observe that the three aforementioned sets of theoretical expressions for H_V and E_V do not appreciably differ from one another; the greatest differences occur at the highest densities reported ($\phi_2 = 0.5$). In general, the expressions which give the best agreement with the data are the void quantities obtained in the Carnahan–Starling approximations, eqs. (52) and (53).

In figs. 3 and 4 we report our simulation results for the *void* nearest-neighbor distribution function H_V at $\phi_2 = 0.2$ and 0.5, respectively. (Again note that we report only a subset of the data obtained.) Included in the figures is the prediction of eq. (52) which is seen to be in excellent agreement with the data.

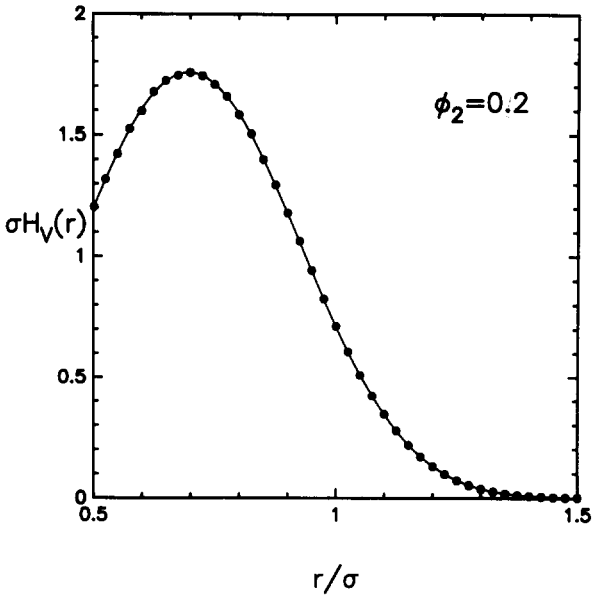

Fig. 3. The dimensionless void nearest-neighbor distribution function $\sigma H_V(r)$ for an equilibrium distribution of impenetrable spheres of diameter σ at a sphere volume fraction $\phi_2 = \eta = 0.2$. Circles are our simulation data and the solid line is the relation (52) obtained in ref. [12]. Here $\eta = \rho\pi\sigma^3/6$ and ρ is the number density.

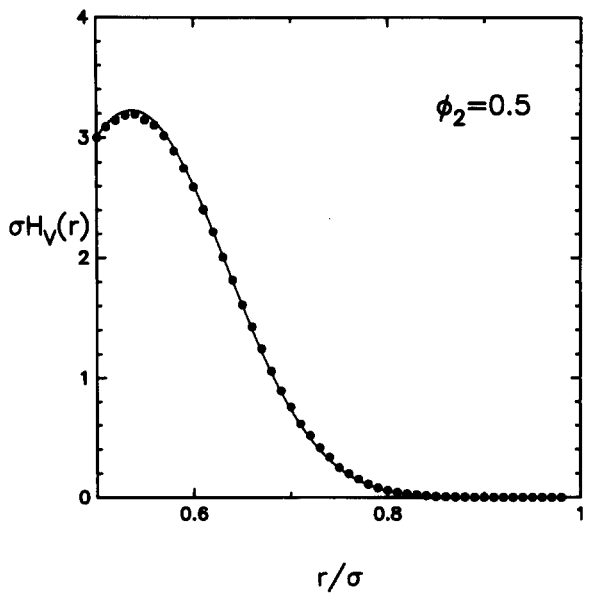

Fig. 4. As in fig. 3 with $\phi_2 = \eta = 0.5$.

At $\phi_2 = 0.2$, the other theoretical expressions (eqs. (37), (46)) are imperceptibly different from eq. (52) on the scale of the figure and hence are not shown. At $\phi_2 = 0.5$, the other expressions, although perceptibly different from (52), are still relatively close to (52) and hence are again not shown. Among the expressions (37) and (46), the relation (46) is generally the most accurate.

In figs. 5 and 6 we give corresponding results for the *void* exclusion probability functions. Included in these figures is the prediction of eq. (53), i.e., E_V in the Carnahan–Starling approximation. Again the other theoretical expressions (38) and (47) are relatively close to (53), with (47) usually being the closest to (53).

Results for $\phi_2 = 0.1$, 0.3 and 0.4 are not shown since they are, not surprisingly, in excellent agreement with the expressions (52) and (53).

Employing our simulation results for $H_V(r)$ and $E_V(r)$, we have determined the conditional pair distribution function $G_V(r)$ using eq. (9). The resulting values of $G_V(r)$ were found to be scattered around the corresponding Carnahan–Starling prediction (eq. (54)). The scatter in the "data" was significantly reduced and agreement with eq. (54) substantially improved as the number of configurations in the simulations for H_V and E_V were increased. This indicates, as expected, that eq. (54) provides an excellent approximation to $G_V(r)$. Since

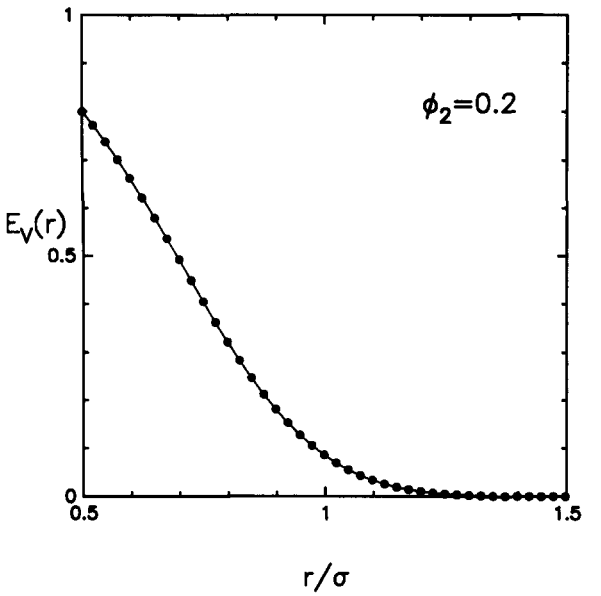

Fig. 5. The void exclusion probability $E_V(r)$ for an equilibrium distribution of impenetrable spheres of diameter σ at a sphere volume fraction $\phi_2 = \eta = 0.2$. Circles are our simulation data and the solid line is the relation (53) obtained in ref. [12]. Here $\eta = \rho\pi\sigma^3/6$ and ρ is the number density.

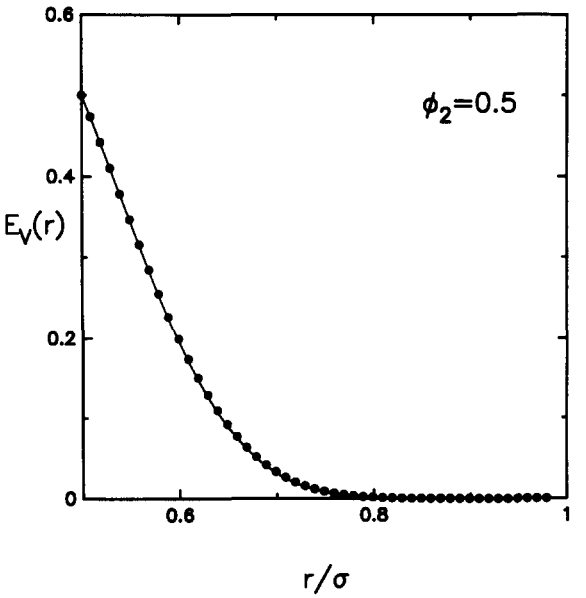

Fig. 6. As in fig. 5 with $\phi_2 = \eta = 0.5$.

reducing the aforementioned fluctuations requires very large amounts of computer time and since eq. (54) is undoubtedly accurate, we do not present such results for $G_V(r)$. Note that $G_V(r)$ in the Percus–Yevick approximation (eq. (48)) underestimates the data, especially at high densities.

6. Results for impenetrable spheres: particle quantities

Our simulation results for the *particle* quantities, H_P and E_P, in the instance of hard spheres is reported here. Again, one of our objectives will be to determine which of the three aforementioned approximations for the particle quantities best agrees with the data. We have carried out simulations for $\phi_2 = 0.1$, 0.2, 0.3, 0.4, and 0.5 but only explicitly report results for $\phi_2 = 0.2$ and 0.5 for the same reasons stated in section 5. We shall use our complete simulation results, however, to calculate the mean nearest-neighbor distance between particles, l, for $\phi_2 = 0.1$, 0.2, 0.3, 0.4 and 0.5. Finally, we shall explicitly test the validity of the relations (26)–(29) derived by Torquato et al. [12].

In figs. 7 and 8 we plot our simulation data for the *particle* nearest-neighbor distribution functions H_P at $\phi_2 = 0.2$ and 0.5, respectively. Included in the

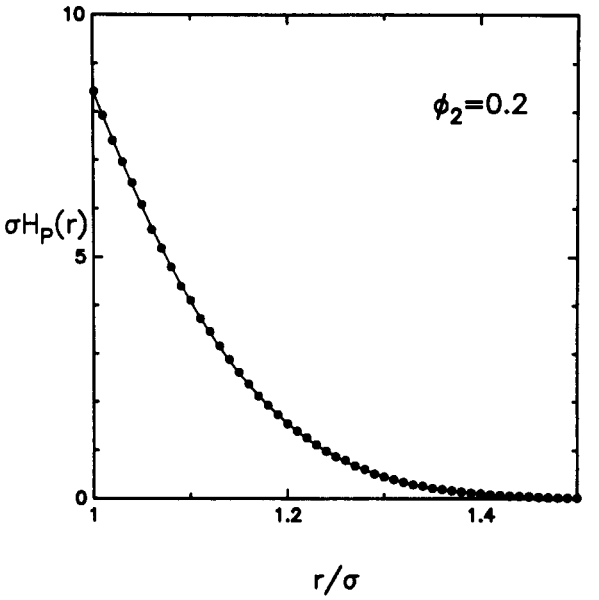

Fig. 7. The dimensionless particle nearest-neighbor distribution function $\sigma H_P(r)$ for an equilibrium distribution of impenetrable spheres of diameter σ at a sphere volume fraction $\phi_2 = \eta = 0.2$. Circles are our simulation data and the solid line is the relation (55) obtained in ref. [12]. Here $\eta = \rho\pi\sigma^3/6$ and ρ is the number density.

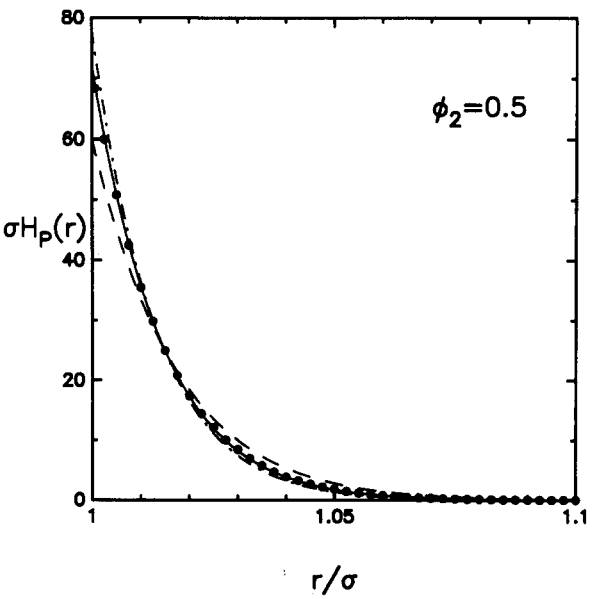

Fig. 8. As in fig. 7 with $\phi_2 = \eta = 0.5$. In addition to the solid line, eq. (55), we have also included eq. (43) (—·—·) and eq. (49) (– – –), all of which were obtained in ref. [12].

figures is the Carnahan–Starling approximation (55) for H_p which is shown to be in excellent agreement with the data. At $\phi_2 = 0.2$, the other expressions, (43) and (49), are numerically close to (55) and hence are not shown. Eqs. (43) and (49) are included in fig. 8 for $\phi_2 = 0.5$, however.

In figs. 9 and 10 we show the corresponding results for the *particle* exclusion probabilities. Again, it is seen that the Carnahan–Starling expression (56) for E_p is in excellent agreement with the data.

We now shall compute the mean nearest-neighbor distance between particles, l, defined by (17). Integrating (17) by parts and using (8) gives the alternative form for hard spheres:

$$\frac{l}{\sigma} = 1 + \int_1^\infty E_p(x)\,dx\,. \tag{66}$$

Eq. (66) is numerically computed using a trapezoidal rule in conjunction with our simulation data for $\phi_2 = 0.1$, 0.2, 0.3, 0.4 and 0.5, and the approximation (56). These results are summarized in fig. 11 where it is seen that theory and

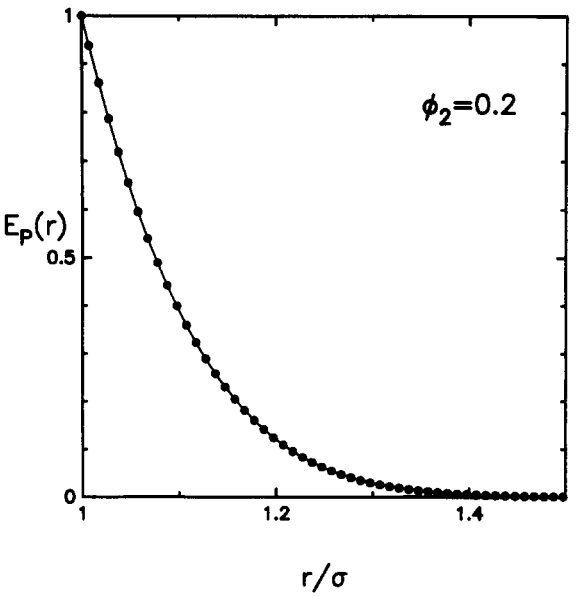

Fig. 9. The particle exclusion probability function $E_p(r)$ for an equilibrium distribution function of impenetrable spheres of diameter σ at a sphere volume fraction $\phi_2 = \eta = 0.2$. Circles are our simulation data and the solid line is the relation (56) obtained in ref. [12]. Here $\eta = \rho\pi\sigma^3/6$ and ρ is the number density.

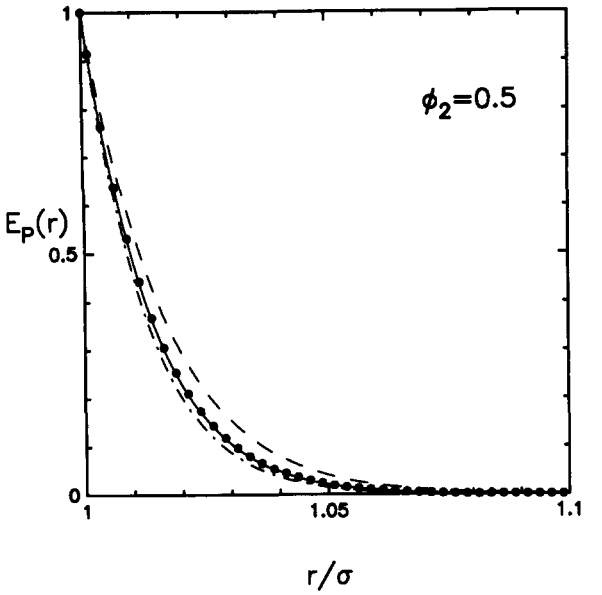

Fig. 10. As in fig. 9 with $\phi_2 = \eta = 0.5$. In addition to the solid line, eq. (56), we have also included eq. (44) (—· —·) and eq. (50) (– – –), all of which were obtained in ref. [12].

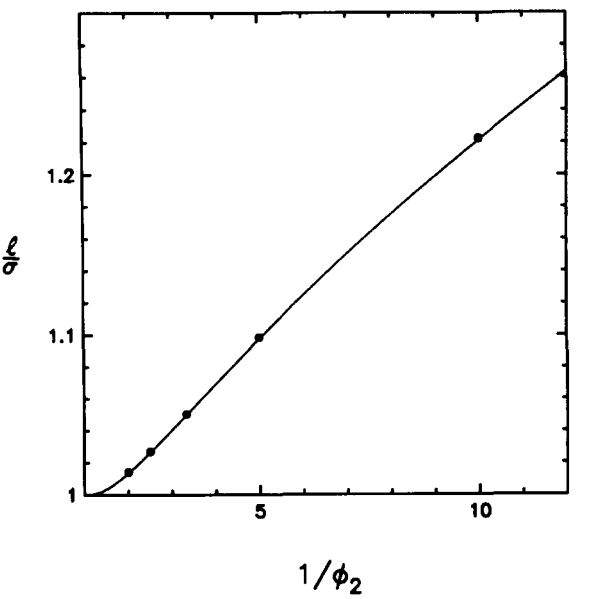

Fig. 11. The dimensionless mean nearest-neighbor distance between particles, l/σ, as a function of inverse sphere volume fraction ϕ_2^{-1} for hard spheres of diameter σ as computed from eq. (66). Circles are obtained from our simulation data and the solid line is obtained using eq. (56).

simulation data are in excellent agreement. Preliminary calculations (not reported here) show that the Carnahan–Starling relations for $E_P(r)$ and $H_P(r)$ will be fairly accurate up to $\phi_2 = 0.6$, thus indicating that its prediction of l (up to $\phi_2 = 0.6$) will also be fairly accurate. For ϕ_2 in the near vicinity of the random close-packing value ($\phi_2^c \simeq 0.64 \pm 0.02$) [2] however, the Carnahan–Starling approximation must necessarily break down since it predicts $\phi_2^c = 1$. Simulation results for $\phi_2 > 0.5$ will be obtained in a future work.

It is of interest to explicitly test the validity of the expressions (26) and (27), which relate the *void* to the *particle* quantities for hard-sphere systems, using our simulation data. The case $\phi_2 = 0.2$ will be examined. At $\phi_2 = 0.2$, we find that the void simulations, among other values, yield $E_V(\sigma) = 0.0841$, $H_V(\sigma) = 0.716$, $E_V(1.1\sigma) = 0.0325$, $H_V(1.1\sigma) = 0.341$, $E_V(1.2\sigma) = 0.010$, and $H_V(1.2\sigma) = 0.129$. Hence, according to relations (26) and (27) we can calculate the corresponding particle quantities and find that $E_P(\sigma) = 1$, $H_P(\sigma) = 8.51$, $E_P(1.1\sigma) = 0.386$, $H_P(1.1\sigma) = 4.05$, $E_P(1.2\sigma) = 0.119$, and $H_P(1.2\sigma) = 1.53$. These predicted values are to be compared with the corresponding direct simulation results: $E_P(\sigma) = 1$, $H_P(\sigma) = 8.53$, $E_P(1.1\sigma) = 0.388$, $H_P(1.1\sigma) = 4.06$, $E_P(1.2\sigma) = 0.121$, and $H_P(1.2\sigma) = 1.54$. It is seen that the *predicted* values from the right-hand sides of eqs. (26) and (27) yield for the particle quantities which are in excellent agreement with the *independently* obtained *simulation* values.

7. Conclusions

We have obtained Monte Carlo simulation results for the *void* and *particle* nearest-neighbor distribution functions and exclusion probabilities for hard-sphere systems up to the volume fraction corresponding to the fluid-solid phase transition. It was generally found that the sets of expressions obtained by Torquato et al. in the Carnahan–Starling approximation gave excellent agreement with the simulation data. How accurate are these expressions expected to be for $\phi_2 > 0.5$, i.e., for $0.5 < \phi_2 < \phi_2^c$, where ϕ_2^c ($\phi_2^c \simeq 0.64$) is the random-close-packing value? Preliminary calculations show that the Carnahan–Starling expressions should still be relatively accurate up to $\phi_2 = 0.6$. In the near critical region, however, these relations clearly break down. At any rate, detailed simulations of the nearest-neighbor functions for hard-sphere systems for $0.5 < \phi_2 < \phi_2^c$ using the algorithm described here will be the subject of a future investigation.

Acknowledgements

The authors would like to thank Binglin Lu for many valuable discussions. The authors also gratefully acknowledge the support of the Office of Basic Energy Sciences, U.S. Department of Energy, under Grant No. DE-FG05-86ER13842.

References

[1] J.L. Finney, Proc. R. Soc. London A 319 (1970) 479.
[2] J.G. Berryman, Phys. Rev. A 27 (1983) 1053.
[3] Y. Song, R.M. Stratt and E.A. Mason, J. Chem. Phys. 88 (1988) 1126.
[4] R. Zallen, The Physics of Amorphous Solids (Wiley, New York, 1983).
[5] J.B. Keller, L.A. Rubenfeld, and J.E. Molyneux, J. Fluid Mech. 30 (1967) 97.
[6] J. Rubinstein and J. B. Keller, Phys. Fluids 30 (1987) 2919.
[7] J. Rubinstein and S. Torquato, J. Fluid Mech. 206 (1989) 25.
[8] J. Rubinstein and S. Torquato, J. Chem. Phys. 88 (1988) 6372.
[9] S. Torquato and J. Rubinstein, J. Chem. Phys. 90 (1989) 1644.
[10] S. Chandrasekhar, Rev. Mod. Phys. 15 (1943) 1.
[11] P. Hertz, Math. Ann. 67 (1909) 387.
[12] S. Torquato, B. Lu and J. Rubinstein, Phys. Rev. A 41 (1990) 2059.
[13] H. Reiss, H.L. Frisch, and J.L. Lebowitz, J. Chem. Phys. 31 (1959) 369.
[14] J.P. Hansen and I.R. McDonald, Theory of Simple Liquids (Academic Press, New York, 1976).
[15] J.M. Haile, C. Massobrio and S. Torquato, J. Chem. Phys. 83 (1985) 4075.